



RESEARCH ARTICLE

STUDYING THE EFFECT OF USING CHITOSAN MODIFIED WITH DIETHYLENETRIAMINEPENTA ACETIC ACID (DTPA) TO OVERCOME SCALE FORMATION IN HEAT EXCHANGERS

¹El Kady, G. M., ²El-Bassousy, A. A. and ^{*}1Mohamed Ali Medan

¹Applied Chemistry Department, Faculty of Science, Al-azhar University

²Analysis and Evaluation Department, Egyptian Petroleum Research Institute (EPRI)

ARTICLE INFO

Article History:

Received 07th December, 2015

Received in revised form

24th January, 2016

Accepted 28th February, 2016

Published online 16th March, 2016

Key words:

Chitin,
Chitosan,
DTPA,
Degree of Deacetylation (DD),
Fouling,
Calcium sulfate scale,
Scale inhibitor.

ABSTRACT

In this work, chitosan and Chitosan-Ethylenediaminepentaacetic acid (DTPA) was prepared, evaluated and applied to inhibit calcium sulfate scale according to the following sequences:

- 1.Extraction and characterization of chitosan from shrimp shells waste.
 - 2.Preparation and evaluation of chitosan-diethylenetriaminepentaacetic acid (DTPA) as scale inhibitor.
 - 3.Make a comparative study of the produced scale inhibitor with other scale inhibitors such as:
 - Ethylenediaminetetraacetic acid (EDTA).
 - Sodium hexameta phosphate (SHMP).
 - 4.Investigate experimentally the effect of the operating parameters such as, **velocity, temperature, water constituents and salt concentration** on calcium sulfate scale formation process
 - 5.Evaluation the performances of these inhibitors and determine their optimal dose for maximum anti-scale effect.
 - 6.An experimental unit was designed and coupled with a data acquisition system for a continuous measuring and monitoring the investigated parameters.
- The results showed that, low molecular mass chitosan samples with DD > 64% and Mw of the major component <10⁴ was obtained by treating the chitin with 50% NaOH at 100 °C for up to 10 h. The antiscalants used in the present work have the following order for reducing calcium sulfate scaling Chitosan-DTPA > EDTA > SHMP.

Copyright © 2016 El Kady et al. This is an open access article distributed under the Creative Commons Attribution License, which permits unrestricted use, distribution, and reproduction in any medium, provided the original work is properly cited.

Citation: El Kady, G. M., El-Bassousy, A. A. and Mohamed Ali Medan, 2016. "Studying the effect of using Chitosan modified with Diethylenetriaminepenta acetic acid (DTPA) to overcome scale formation in heat exchangers", *International Journal of Current Research*, 8, (03), 27098-27114.

INTRODUCTION

That of the most important problems facing many industrial fields such as petroleum, desalination plants, sugar industry, cements industry and phosphoric acid plants; The accumulation of unwanted deposits on heat transfer surfaces (heat exchangers, steam generators, boilers, cooling towers, pipes, etc.) leading to an increase in the resistance to heat transfer and subsequent loss of thermal exchange capacity of the heat transfer equipment. These deposits are usually known as "fouling". The foulant may be crystalline, biological material, the products of chemical reactions including corrosion, or particulate matter. The character of the deposit depends on the fluid (liquid or gas) passing through the heat exchanger (Bipan Bansal *et al.*, 2008; Lisitsin *et al.*, 2005; Heitmann, 1990).

Fouling is generally classified in six different categories crystallization, particulate, reaction, corrosion, biological, and solidification (Senthilmurugan *et al.*, 2010; Bott, 1995). Out of all these types, crystallization fouling is the one which probably has the most detrimental effect on the industry around the world. Crystallization fouling is caused by the crystallization of a dissolved species from the process solution onto a heat transfer surface. It occurs when the concentration of the dissolved species in the process solution exceeds its solubility limit. There are various conditions which can lead to super-saturation (Bipan Bansal *et al.*, 2008):

- Solution of normal solubility salts cooled below solubility temperature.
- Solution of inverse solubility salts heated above solubility temperature.
- Solution evaporated beyond the solubility limits of the dissolved species.

*Corresponding author: Mohamed Ali Medan,

Applied Chemistry Department, Faculty of Science, Al-azhar University

- Mixing of different streams leading to supersaturated conditions.
- Change in pH of process solution.

Calcium sulfate is precipitated from saline water upon heating and there are three chemical variances of calcium sulfate that can be formed in sea water: anhydrite CaSO_4 , hemihydrate $\text{CaSO}_4 \cdot 1/2\text{H}_2\text{O}$, and dihydrate $\text{CaSO}_4 \cdot 2\text{H}_2\text{O}$ (gypsum). Dihydrate is the most stable form at low temperatures while anhydrite is formed at higher temperatures. The solubility of calcium sulphate in water is shown in Fig. 1 as a function of operating temperature (Lisitsin *et al.*, 2005). At temperatures higher than 40°C , the solubility of calcium sulphate decreases with increasing temperature for the ordinary solid phases. The solubility of calcium sulphate is strongly affected by the presence of other ions in the system. The solubility increases with increasing concentrations of the other substances in the solution. Scale inhibition effectiveness depends on the capability of an additive to interfere with the scale formation steps, either with the step of nucleation or with that of crystal growth. Various inhibitors are considered to act according to one (or more) of the following main mechanisms of interference with crystal growth: (i) threshold effect (i.e. influencing the initial clustering process of the proto nuclear), (ii) crystal distortion effect, (iii) dispersion and (iv) chelation (Senthilmurugan *et al.*, 2010; Darton, 2000). Chitosan (CTS) is a partially N-deacetylated derivatives of chitin, which is commonly found in the shells of insects and crustaceans, as well as cell wall of some fungi, and is known as the second most abundant biopolymer in nature after cellulose (Muzzarelli, ?; Muzzarelli *et al.*, 1986). The chemical structure of CTS chain $(\text{C}_6\text{H}_{11}\text{NO}_4)_n$ is shown in Fig. 2. CTS has a mass of 161 g per unit monomer, and has a concentration of amino group ($-\text{NH}_2$) of 6.21 mmol/g if it is completely deacetylated. The adsorption of transition metals on CTS is known to be mainly effected via coordination with the unprotonated amino group (Monteiro and Airoidi, 1999).

Experimental Work

Materials and Method

Materials

Frozen shrimp shells, were stored in a freezer before use. Diethylenetriaminepentaacetic acid (DTPA), hydrochloric acid, acetic acid, acetone, sodium hydroxidewere obtained from El-Nasr for chemicals Co. All chemicals of commercial grade.

Method

Chitin and Chitosan Extraction from Shrimp Shell

Step 1: sample Preparation

The shrimp shells were obtained from a local source in Egypt. The shells were cooked in a presto pan for 10 min, followed by filtration, washing, drying and weighing.

Step 2: deproteinization

Crushed and dried shrimps were placed in 1000 ml beaker and soaked in 5% sodium hydroxide (w/v 1:8) for two hours at 60°C

in order to dissolve the proteins and other organic materials thus isolating the crude chitin. After the reaction, the solution was colored and frothy, therefore, the sample was washed repeatedly with water until most of the color and frothing disappeared and the resulting solution was near neutral.

Step 3: decolouration

Deproteinized shells were treated with acetone at room temperature for 10 h with stirring to remove pigments. The washed shells were filtered and dried in a vacuum oven at 60°C until constant weight.

Step 4: demineralization

The grounded shell is demineralized using 1% HCl with four times its quantity. The sample was allowed to soak for 24 h to remove the minerals (mainly calcium carbonate). The prawn shells were then washed several times with water to remove CaCl_2 and other water soluble impurities.

Step 5: deacetylation of chitin

Chemical deacetylation was achieved by treatment of extracted chitin with 50% sodium hydroxide (NaOH) solution at elevated temperature, 80°C using a solid to solvent ratio of 1:5 (scheme 1). After the reaction the material produced was washed several times with distilled water until near to neutral pH and dried at 60°C in a vacuum oven until constant weight.

Preparation of Chitosan-DTPA (DTPA-functionalized chitosan)

Chitosan (5 g, 31 mmol) was dissolved in a 10% (v/v) aqueous acetic acid solution (100 mL). The solution was diluted in methanol (400 mL). DTPA bisanhydride (33.23 g, 93 mmol) was suspended in methanol (100 mL) and added to the chitosan solution and stirred for about 24 hours at room temperature to allow the reaction with the chitosan to proceed. After filtration, the precipitate was mixed with ethanol and stirred for another 12 hours. After filtering again, the precipitate was mixed with a 0.1 M NaOH solution (nearly 1 L). More NaOH (in total equivalent to 0.2 M NaOH) had to be added gradually to the reaction mixture in order to effectively reach a pH of 11. This can be explained by the strong buffering effect of DTPA. It is however important not to bring functionalized chitosan into direct contact with the 0.2 M NaOH solution in order to avoid amide hydrolysis. The reaction mixture was stirred for another 12 hours. Non-reacted DTPA is converted into its sodium salt and thus dissolves in the aqueous phase. Next, the functionalized chitosan was filtered off. Because of the high viscosity of the reaction mixture, filtration was very slow. It was therefore important to find the right pore size of the sintered filter glass to achieve acceptable flow. The precipitate was washed several times with demineralized water, each time followed by centrifugation until the supernatant had a neutral pH. The precipitate was then mixed with a 0.1 M HCl solution and washed repeatedly with demineralized water until the pH of the washing water was neutral. After a stirring step in ethanol, followed by filtration, the product was dried in a vacuum oven at 40°C for 48 hours to give a white solid.

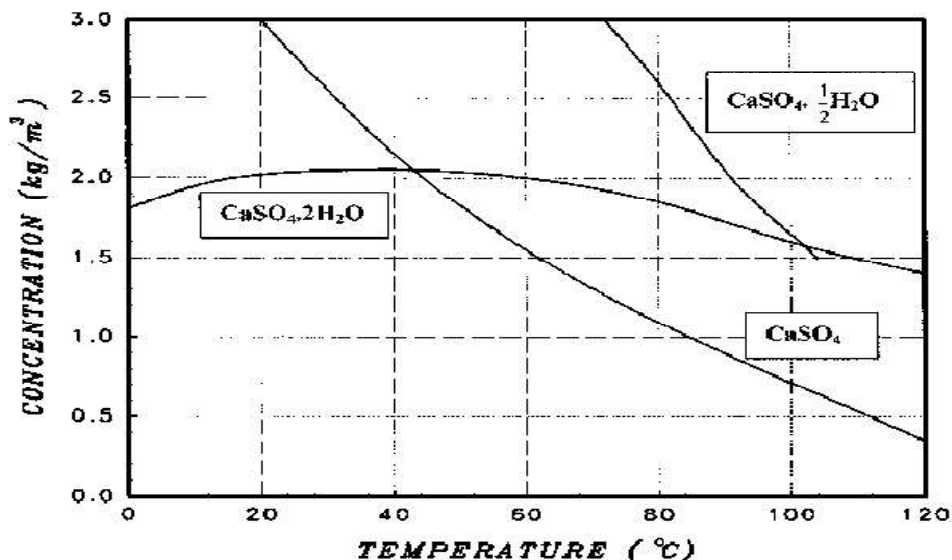


Figure 1. Solubility of calcium sulphate in water as a function of temperature (Faizur Rahman, 2013)

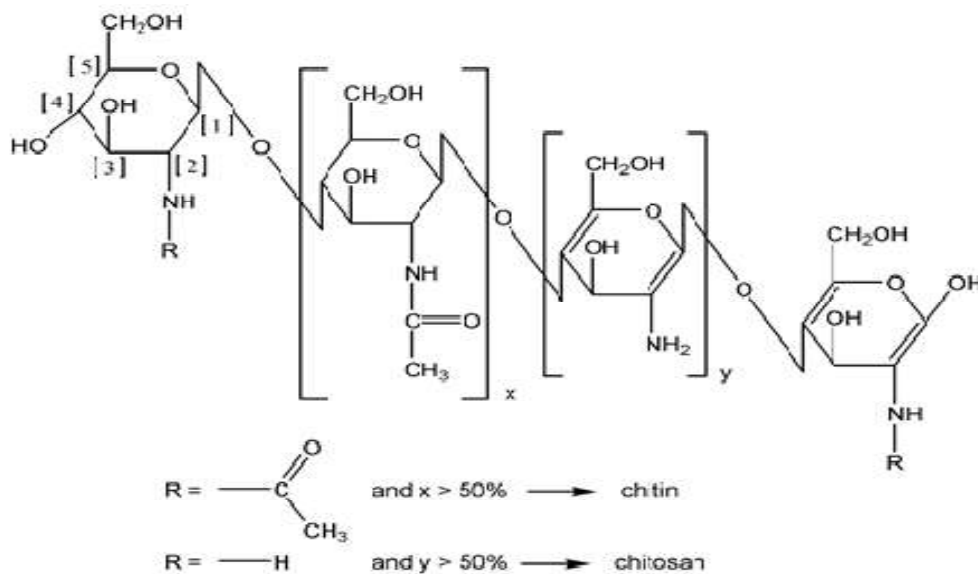
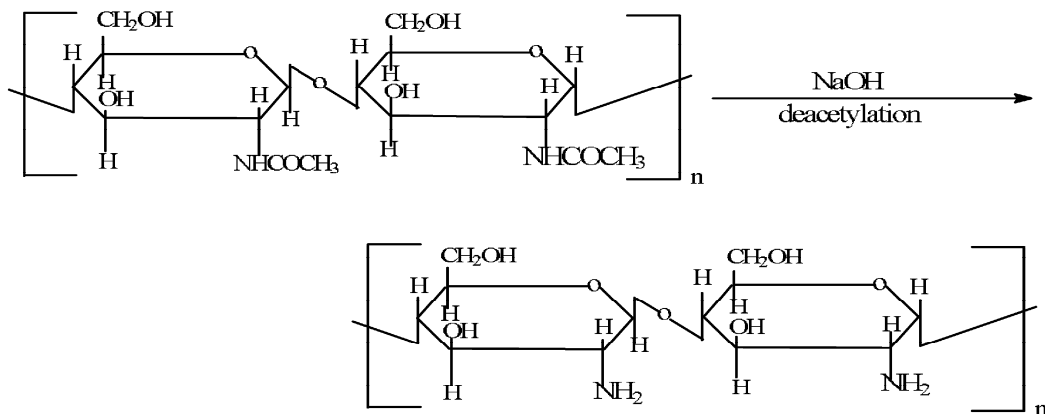


Figure 2. Structure of chitin and chitosan (reproduced from Ref. [51] by permission of Elsevier Science, Amsterdam)



Scheme 1.

Chitosan and Chitosan-DTPA Characterization

Chitosan Characterization

Fourier Transform Infrared Spectroscopy (FTIR)

Chitin and chitosan samples were ground to a very fine powder with KBr and dried thoroughly. The dried mixture was pressed under vacuum in a mold to form a KBr disc containing the sample. FTIR spectroscopic measurements were also performed on films of soluble chitosan. Chitosan samples with a low degree of deacetylation (DD) were dissolved in 20% HCl while samples with a DD of 50% and above were dissolved in a 1% solution of acetic acid. Subsequently, the films were cast on plastic trays and left to dry at room temperature. Neutralization of protonated $-NH_2$ before obtaining the FTIR spectra was done by leaving the dried films in 1% NaOH solution for 24 h. This was followed by repeated washing steps using distilled water and a drying step under vacuum at 40 °C for 12 h or until constant weight. FTIR spectra were recorded using a Perkin Elmer FTIR Spectrometer over the frequency range of 4000-625 cm^{-1} . 16 scans were accumulated at a resolution of 4 cm^{-1} . FTIR spectroscopy was also used to estimate the degree of deacetylation (DD) of chitosan. The DD of the chitosan samples was calculated from the absorbances at 1658 and 3450 cm^{-1} according to the following equation:

$$DD (\%) = 100 - [(A_{1658} / A_{3450}) \times 115]$$

where A_{1658} and A_{3450} are the absorbance at 1658 cm^{-1} of the amide band as a measure of the N-acetyl group content and the absorbance at 3450 cm^{-1} of the hydroxyl band as an internal standard to correct for film thickness.

The band ratio method of selected bands from their FTIR spectra was also used to determine the DD of the chitosan samples. The bands at 1318 and 1382 cm^{-1} were chosen as measuring and reference bands, respectively. To measure the peak intensities for these two bands, baselines were drawn between the 1350 - 1280 cm^{-1} and 1490 - 1350 cm^{-1} wavenumbers, respectively. The DD was determined by using the following equation:

$$A_{1318} / A_{1382} = 0.3822 + 0.03133 DA$$

NMR spectroscopy

Chitosan samples were analyzed by proton Nuclear Magnetic Resonance (1H NMR) Spectroscopy on a Bruker Avance DRX-500 (500 MHz) spectrometer. The samples for NMR were prepared by dissolving 7-10 mg of chitosan in 1-10% DCl in D_2O , depending on the solubility of the sample. The degree of deacetylation was calculated by using integrals of the peak of the proton of the CH group connected to nitrogen moiety at 3.11 ppm of the deacetylated monomer unit (H1-D) and of the peak of the three protons of the acetyl group (H-Ac) at 1.99 ppm of the acetylated monomer unit as shown in the following equation.

$$DD = \frac{(\text{area of } 3 \times H1 - D)}{(\text{area of } 3 \times H1 - D + \text{area of } H - Ac)} \times 100$$

X-ray diraction

X-ray diraction analysis (XRD) was applied to detect the crystallinity of the extracted samples of chitin and their corresponding chitosan. A Scintag powder diffractometer was used for this purpose between 2θ angles of 5° and 40°. Ni-filtered Cu $K\alpha$ -radiation was used as the X-ray source. The relative crystallinity of the polymers was calculated by dividing the area of the crystalline peaks by the total area under the curve.

Ash Value

To determine the ash value of chitosan, 2.0 g of chitosan sample is placed into previously ignited, cooled, and tarred crucible. The samples are heated in a muffle furnace preheated to 650 °C for 4 hr. The crucibles are allowed to cool in the furnace to less than 200 °C and then placed into desiccators with a vented top. Percentage of ash value is calculated using the following equation.

$$\% \text{ Ash} = \frac{(\text{weight of residue, g})}{\text{sample weight, g}} \times 100$$

Moisture Content

Moisture content of the prepared chitosan was determined by the gravimetric method (7). The water mass was determined by drying the sample to constant weight and measuring the sample after and before drying. The water mass (or weight) was the difference between the weights of the wet and oven dry samples.

$$\% \text{ of moisture content} = \frac{(\text{wet weight, g} - \text{dry weight, g}) \times 100}{\text{wet weight, g}} \text{Viscosity}$$

Measurements

The viscosities of all prepared chitosan samples (except the insoluble samples) were measured using an Ostwald capillary viscometer and the intrinsic viscosities were determined, the solvent was 5% acetic acid and 0.1 M KCl the obtained intrinsic viscosity was used to calculate molecular weight for the prepared samples from the Mark-Houwink-Sakurada relation:

$$(\eta) = KM a$$

where M is viscosity average molecular weight; K and a are constants, whose values depend on the polymer type and the chosen solvent. As was shown in (Marianna Laka and Svetlana Chernyavskaya, 2006; Terbojevidh and Cosani, 1997) for chitosan and the solvent 0.5 M AcOH - 0.2 M NaOAc, these constants are 3.5×10^{-4} and 0.76, respectively, and they do not depend on the deacetylation degree.

Application Experiment

Experimental Set-Up

The experimental setup used in the present work is shown in Fig. 3 and 4. This setup consists of a closed-circulation loop and a test section as follows:

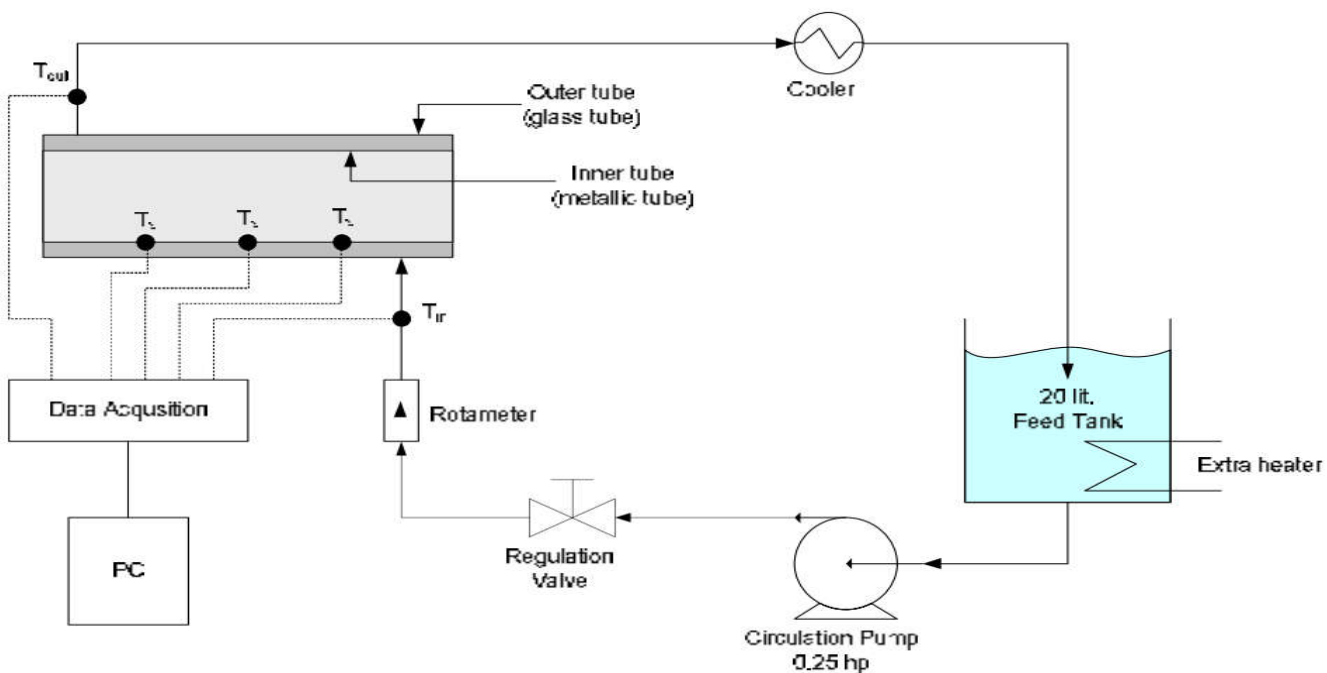


Figure 3. The circulation test loop of the experimental setup

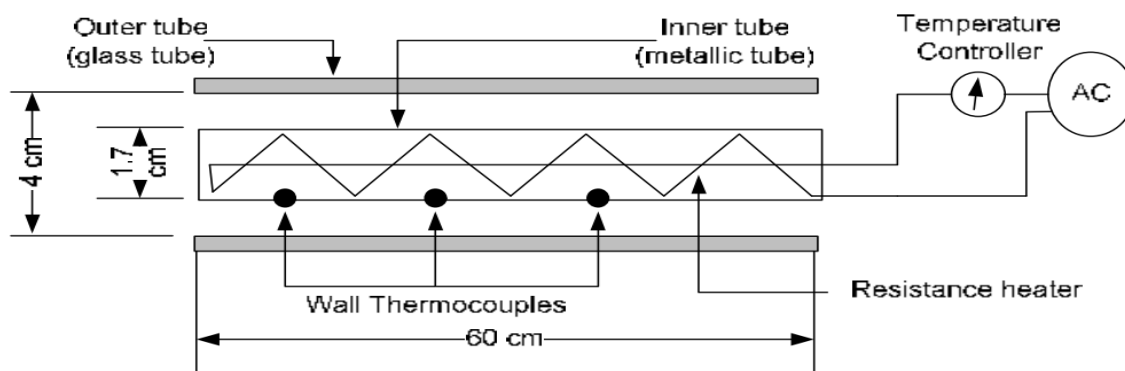


Figure 4. The test section with its cartridge heater

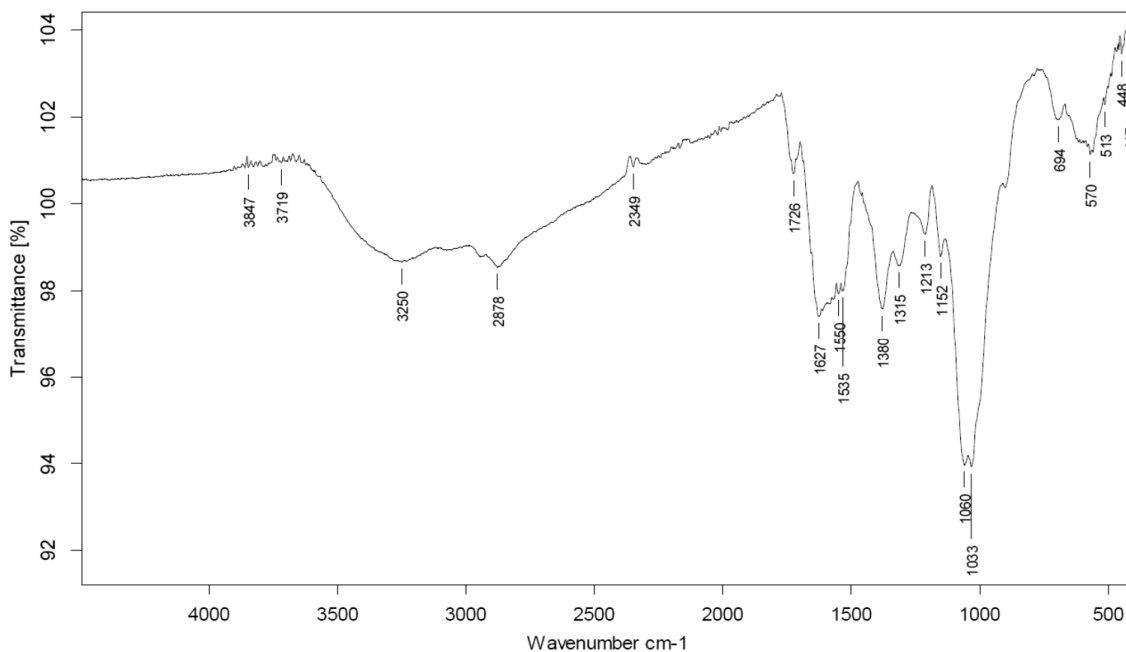


Figure 5. IR-spectrum Chitosan – DTPA

(a) The Circulation Loop

The circulation loop, shown in Fig.3 consists of the feed tank with 20 liters capacity for the preparation and adjusting the test solution. The tank is also connected to a level controller to compensate for any water evaporation losses during the whole period of experimental runs. The loop has also a centrifugal pump of 0.25 hp for circulating the flow inside the test section according to the desired flow rate which is indicated by the flow meter reading (the flow meter used is a rotameter of model FL-73, produced by Omega Engineering, inc.). The loop is fitted with a cooler to adjust the temperature of the exit solution from the test section before entering into the feed tank. An extra heater is also inserted in the feed tank to adjust the input temperature of the test solution.

The temperature measuring devices mainly the thermocouples and the data acquisition system with a P.C. are also connected to this loop as will be explained later.

(b) The Test Section

The test section shown in Fig.4 is an electrically heated metal tube (stainless steel) with 1.7 cm outside diameter and 60 cm length while its wall thickness is 0.25 cm. Inside this tube, an electric heater of the cartridge type (home made with a power of 1 KW) is inserted longitudinally as shown in Fig. 4. The metallic tube itself is enclosed in a wider glass tube of 4 cm inside diameter and 60 cm length while its thickness is 0.5 cm. The test fluid is forced to flow through the annulus between the metallic tube and the glass one. Hence visual observations are always possible with this configuration. The scale deposits with this type of test rigs are formed on the outside surface of the investigated metallic tube. Hence, for each run, the weight of the test section, the metallic tube, was obtained at the start and at the end of each run to find the weight of the fouling deposits (using an accurate mettler balance of model no. PL 1200 with readability of 0.01 and capacity of 1200 g) from which the fouling resistance "R_f" was also calculated (as will be explained later).

(c) Temperature Measurements

As previously mentioned, thermocouples are used in the present work for temperature measurements in order to be easily interfaced with the data acquisition unit. Six thermocouples of the type K (nickel-chrome its error is ± 0.7 °C) are actually used in our experimental work. Three thermocouples are used to measure the surface temperature of the metallic test section and one to measure the temperature of the test solution in the feed tank and two are used to measure the input and output temperatures of the test fluid.

(d) Data Acquisition

A data acquisition system was used to record, store, and display real time measurements of temperature. The system used consists of a data acquisition board and a personal computer with a hard disk. The data acquisition board is Pico Technical limited model TC-08, with 8 channel thermocouple to transfer

data directly from the Analog/Digital converter to the memory in the PC.

Experimental Parameters

The experimental parameters affecting scale formation and fouling phenomena which are considered in the present investigation are:

Duration Time

Fouling is a dynamic process in which the fouling resistance changes with time. Thus, in the present study the weight of the deposit was measured at various intervals until a steady state value is achieved.

Feed temperature of the fluid

The feed (input) temperature was varied via an electric heater connected to the feed tank. It is worth mentioning that the changing this feed temperature will lead to corresponding change in both output temperature of the test fluid and the surface temperature of the test section which has significant role in the scale formation process. Applied feed temperatures are 40, 50, and 60 °C.

Fluid velocity

The fluid velocity is an important parameter in scale formation processes; hence various flow rates are investigated in the present work and their corresponding velocities and Reynolds numbers were obtained in order to discuss their effects on the fouling deposit. Range of velocities applied in this work is from 0.043 to 0.13 m/s.

Concentration of the fouling salts

Different concentrations of the fouling salts are used in the present work (1000, 3000, 5000 and 7000 ppm for calcium sulfate and calcium carbonate and 100, 200 and 300 for both magnesium hydroxide and barium sulfate).

Scale Inhibitor

Scale inhibitor can prevent the precipitation of scale forming salts by preventing formation of crystals larger than the critical size (preventing nucleation) and by surface modification of those crystals which do form. The surface modification of the crystals causes them to distort as they grow. This distortion can slow and actually stop the growth of the usually highly-ordered crystals. Several types of scale inhibitors are commercially available now and the proper selection of a scale inhibitor depends upon the water chemistry and system design.

- Scale inhibitors may act in one or more of a number of ways:
- It may destroy the activity of the foulant.

It may physically affect the fouling process by changing the physical interaction between the foulant and the heat exchanger surface. The additive may modify the nature of the deposit

residing on the surface so that it is more susceptible to the removal surface. It may react chemically with the fouling species to modify its fouling potential. Three scale inhibitors were used and tested in the present work to investigate their effects on calcium sulfate deposition. The scale inhibitors are:

- Prepared Chitosan – DTPA;
- Sodium Hexametaphosphate (SHMP), and
- Ethylenediaminetetraacetic acid (EDTA).

The dose concentrations of these scale inhibitors used varied from 1 ppm to 3 ppm in the present study.

RESULTS AND DISCUSSION

Extraction of chitosan from prawn shells

The proportions of the various components obtained at the various stages of the extraction process are given in Table 1.

Step 1: washing with water

The frozen shells were washed with water and it was found that the amount of dried prawn shells left after washing and then drying was 32 wt%. This weight loss is attributed to removal of water and residual prawn flesh.

Step 2: deproteinization

The dried shells obtained after washing in Step 1 were treated with 5% NaOH to remove proteinaceous components together with lipids and pigments. This removed 36 wt% of the material from the prawn shells.

Step 3: decolourisation

The dried shells obtained after Step 1 and Step 2 in experiments were washed with acetone to remove organic material. This removed a small amount of material (14 wt%).

Step 4: demineralization

The decolorized prawn shells were treated with HCl to remove inorganic minerals, mainly CaCO₃. The concentration of HCl used was 1%. The weight loss at this stage was 14.6%. The amount of chitin obtained from the prawn shells ~ 26% based on the dry weight.

Step 5: Chitin deacetylation

The chitin obtained after Step 4 was deacetylated using 50% w/v NaOH. The amount of chitosan obtained was 25 wt% of the original weight of the dried prawn shells.

Preparation of Chitosan – DTPA

Chitosan was functionalized by Diethylenetriaminepentaacetic acid (DTPA). The results showed that, the yield of Chitosan – DTPA was 24% (3.92 g; 7.4 mmol). IR Fig. 5: 3250 cm⁻¹ broad band; O–H stretch + N–H stretch, 2878 cm⁻¹ C–H stretch, 1726 cm⁻¹ C=O stretch, carboxylic acid, 1627 cm⁻¹ C=O stretch, amide, 1380 cm⁻¹ symmetric vibration COO, 1033 cm⁻¹ C–N

stretch, primary amine. The degree of functionalization of the amine groups of chitosan was calculated to be 94% on the basis of the nitrogen analysis results. This value is much higher than the value reported by Nagib *et al.* (22%) (Knudsen, 1990).

Characterization of chitin and chitosan

Fourier Transform Infrared Spectroscopy (FTIR)

The FTIR spectra of powdered prawn shells, chitin, chitosan and commercial chitosan are presented Fig. 6. The FTIR spectrum of chitin, presented in Fig. 6 (b), includes absorbance bands around 3450, 3262, 3114, 2960, 2930, 2888, 1658, 1628, 1560, 1418, 1382, 1318, 1260, 1204, 1158, 1118, 1074, 1026, 952 and 896 cm⁻¹. This is consistent with the structure of α -chitin. In addition there is splitting of the amide I band in the chitin spectrum to give two peaks at 1658 cm⁻¹ which is attributed to the occurrence of intermolecular hydrogen bonds CO...HN and at 1628 cm⁻¹ due to the intramolecular hydrogen bond CO...HOCH₂ and is characteristic of α -chitin. The bands due to NH stretching at 3262 cm⁻¹ and 3114 cm⁻¹ are also characteristic of the α -chitin spectrum. The bands around 1798, 1420 - 1430 and 876 cm⁻¹ in Fig. 6 (a) for the powdered shells are due to mineral (CaCO₃) are not present in chitin after demineralization with 1% HCl while these absorbance are present if demineralization is carried out using 0.5% HCl. The absence of a peak around 1540 cm⁻¹ indicates that protein has been removed. The FTIR spectrum of chitosan (Fig. 6 (c)) shows extra bands in the region 1606-1566 cm⁻¹ due to primary amine groups while the absorptions at 3450, 3262, 3114 and 1658 cm⁻¹ due to amide groups are missing from the deacetylated chitin while absorption at 1632 cm⁻¹ due to -NH₂ deformation of primary amines appears. Absorption at 3398 cm⁻¹ appears due to -NH₂ stretching absorption in amines in chitosan.

NMR spectroscopy

The ¹H NMR spectra of the sample is given in Fig. 7.

X-ray diffraction (XRD)

X-ray diffraction (XRD) patterns of the obtained chitosan are illustrated in Fig. 8. The XRD pattern of chitosan exhibits broad diffraction peaks at 2 θ = 10° and 21° which are typical fingerprints of semi-crystalline chitosan.

Ash Value

Chitosan sample had low ash content, is 1.20 %, indicating the effectiveness of the demineralization step in removing minerals. It is reported (Wang and Kinsella, 1976) that commercial chitosan contain ash about 1.18%. Molecular weight of the prepared chitosan is 165394 g/mole determined by the reported process (Marianna Laka and Svetlana Chernyavskaya, 2006; Terbojevidh and Cosani, 1997).

Moisture Content

The results shows that the prepared Chitosan contains moisture in the range 1.0-1.30% depending on the season, relative humidity and intensity of sun light.

Table 1. The proportions of the various components obtained at the various stages of the extraction processes

Wt. (g)		Wt. (g)		Wt. (g)		Wt. (g)	
Before	after	before	after	before	after	before	after
Deproteinization		Decolourization		Deminerlization		Deacetylation	
20	12.7	12.7	8.2	8.2	7.1	7.1	5.2
Weight loss after each process							
7.3g (36.5 %)		4.5g (22.5 %)		1.1g (5.5 %)		1.9g (9.5 %)	

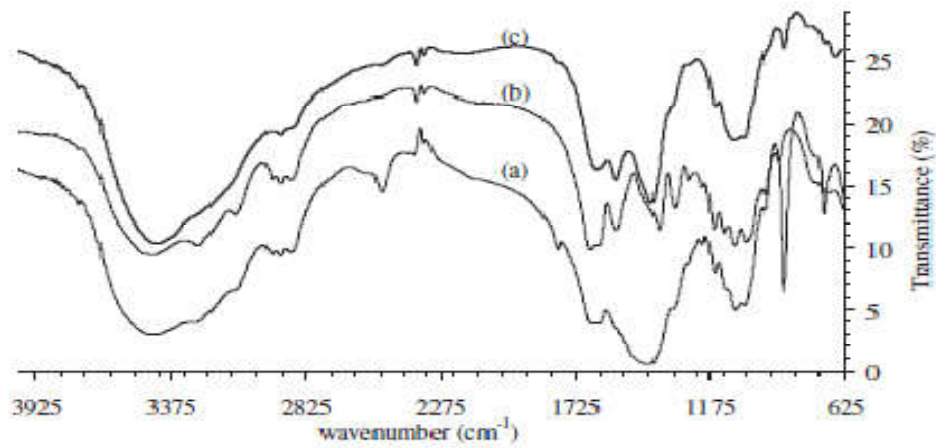


Figure 6. IR spectra of (a) powdered prawn shells (b) extracted chitin and (c) chitosan from prawn shells

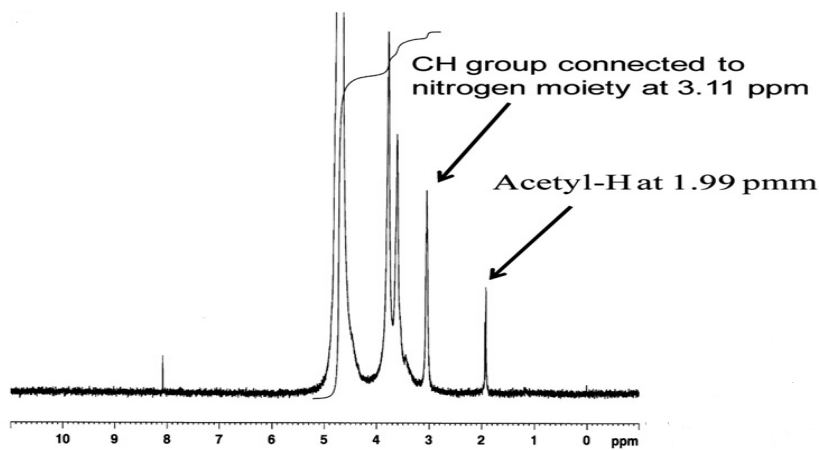
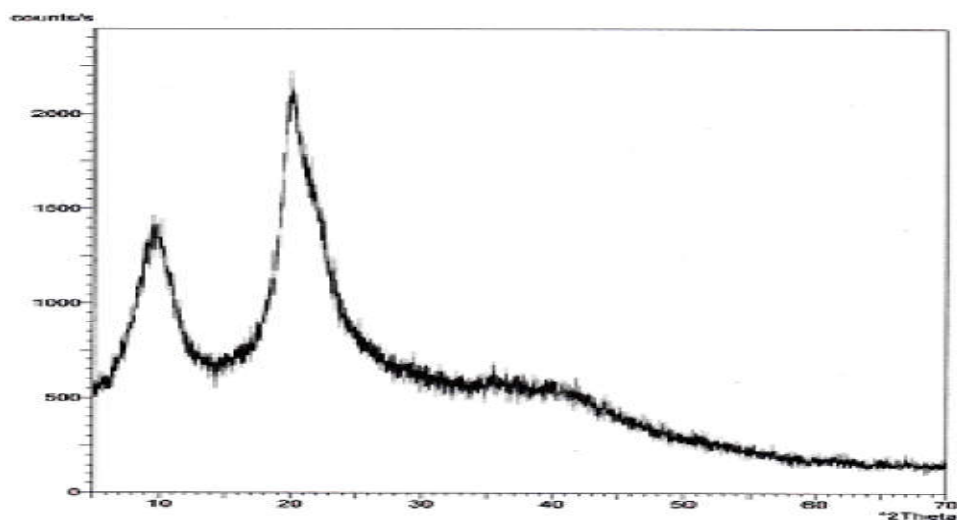
Figure 7. ¹H NMR spectra of chitosan from prawn shells

Figure 8. XRD diffractogram of prepared chitosan

Table 2. Physicochemical and functional properties of the prepared chitosan

Yield %	Moisture %	Ash %	DD %	M.wt. (g/mol)
14.9	1.25	1.2	75	165394

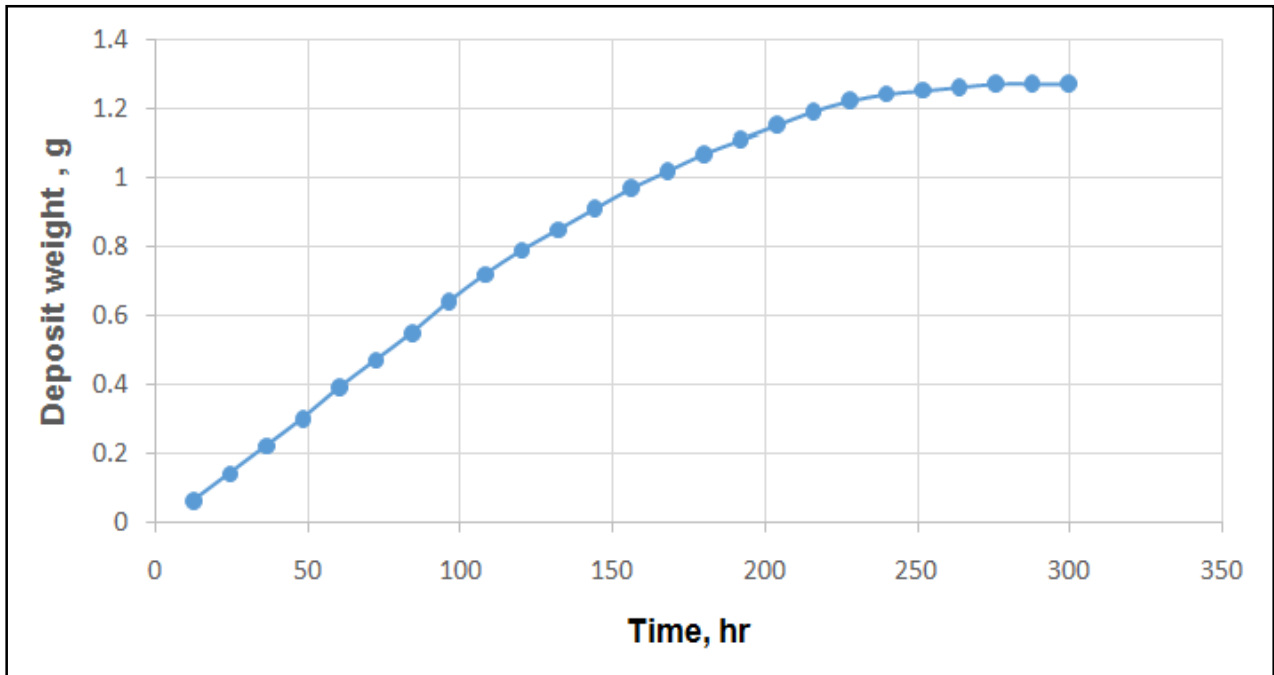


Figure 9. The Change of Deposit Weight with Time. Fixed conditions: $T = 50\text{ }^{\circ}\text{C}$, $\text{pH} = 8$, $u = 0.13\text{ m/s}$, $\text{Re} = 3000$, $q = 31\text{ kW/m}^2$ and CaSO_4 Concentration = 3000 ppm

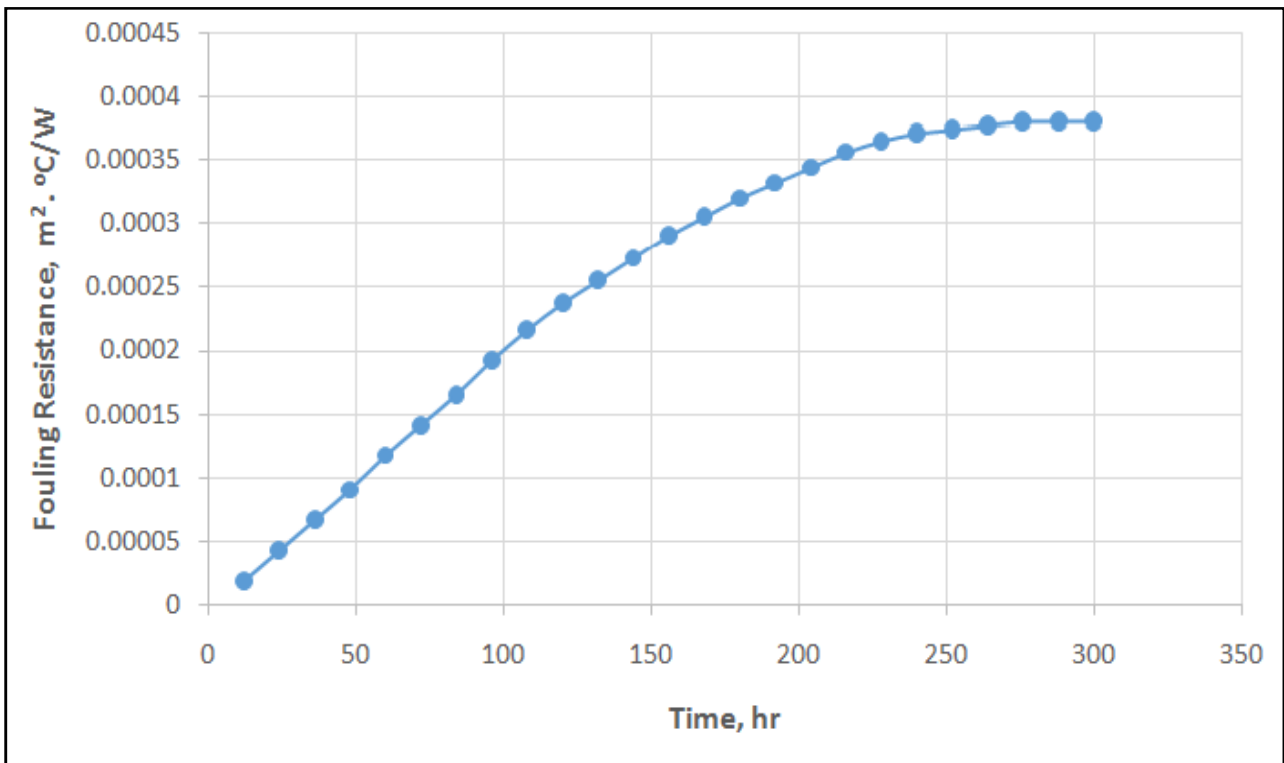


Figure 10. The Change of Fouling Resistance with Time

There is no significant difference in the % moisture content between the reported data elsewhere 1-1.30% and the data obtained from the prepared chitosan (1.25%). According to KFDA (KFDA, 1995) the moisture content of chitosan powder should be below 10%. Several factors during production, including high temperature, concentration of alkali, reaction time, previous treatment of the chitin, particle size, chitin concentration, dissolved oxygen concentration and shear stress may influence the MW of CSs (Hasson and Perl, 1981; Gazit and Hasson, 1975). The following table shows the results of physicochemical and functional properties of the prepared chitosan.

Fouling Study of Calcium Sulfate

Effect of Duration Time

As we know, fouling is a time dependent process, hence in these experiments; various runs were carried out at different intervals and the other parameters were kept as follows:

Input Temperature	:	50 °C
Heat Flux	:	31 KW/m ²
pH	:	8
Fluid Velocity	:	0.13 m/s
Re NO.	:	3000

As shown in Fig. 9, the fouling deposit increases with time until it reaches its steady state value after 300 hours. This fouling curve is very similar to those reported in literature (Knudsen, 1990) and it is usually known as the asymptotic curve. Fig.10 show the results of the fouling resistance. This result is in agreement with Al-Jalil (1998).

Effect of calcium sulfate concentration

Some preliminary experiments were carried out to check the concentration level of calcium sulfate that will be covered. From these experiments, it is found that the deposit begins to form at 1000 ppm. According to these results, the concentration of calcium sulfate was changed from 1000 ppm to 7000 ppm. It is not practical to use concentrations more than 7000 ppm. The other parameters were kept constant as follows:

Input Temperature	:	50 °C
Heat Flux	:	31 KW/m ²
pH	:	8
Fluid Velocity	:	0.13 m/s
Re NO.	:	3000

It is clear from Figs. 11 and 12 that, the fouling deposit and resistance of calcium sulfate are increases by increasing its concentration in the test fluid. Similar results are obtained by Al-Jalil (1998), Bansal *et al.* (2000) and with Najibi *et al.* (1999).

Effect of Fluid Temperature

The fluid temperature plays an important role in scale formation due to its effect on the supersaturation of the fouling salt especially those salt (like calcium sulfate) which have inverse solubility behavior (Knudsen, 1990; Monteiro and Airoldi, 1999). Hence, in these experimental runs, the feed

solution (or input) temperature was varied from 40 °C to 60 °C with the help of the extra heater fitted to the main feed tank (in the experimental set-up). This temperature range was selected at that level to avoid the formation of boiling bubbles at the surface of the test section. The other parameters were kept constant at the following levels:

CaSO ₄	:	1000 ppm
Duration Time	:	72 Hours
Heat Flux	:	31 KW/m ²
PH	:	8
Fluid Velocity	:	0.087 m/s
Re NO.	:	3000

As shown in Figs. 13 and 14, the scale deposit increases and fouling resistance as the feed solution temperature increases due to its effect on the supersaturation of calcium sulfate as expected. It is worth mentioning that, while the feed solution temperature was varied from 40 °C to 60 °C, the surface temperature (as recorded by the data acquisition system) ranged from 52.54 °C to 72.46 °C. As a result of the higher temperature, the reaction rate constant and the supersaturation (CaSO₄ has a decreasing solubility with increasing temperature) increased (Bansal *et al.*, 2000). This result is in agreement with Al-Jalil (1998), Bansal *et al.* (2000) and with Najibi *et al.* (1999).

Effect of Fluid Velocity

No doubt that, the fluid velocity is an important parameter in the scale formation processes. It can either enhance the diffusion of the foulant species towards the heating surface or accelerate the removal of scale deposit from it. Hence, in the present work, the flow velocity of the test fluid was investigated at 0.043, 0.087 and 0.13 m/s (corresponding to Reynolds number of 1000, 2000 and 3000) which is still in the laminar region. The other parameters were kept constant during each run as follows:

CaSO ₄ Concentration	:	3000 ppm
Duration Time	:	72 hours
Heat Flux	:	31 KW/m ²
PH	:	8
Input Temperature	:	50 °C

As shown in Figs. 15 and 16, the weight of scale deposit decreases by increasing the flow velocity which is ascribed to the increase in the removal rate conducted by the flowing fluid as also reported by others in this field (Knudsen, 1990; Yiantsion *et al.*, 1995). This result is in agreement with Al-Jalil (1998) and with Bansal. It is worth mentioning that, higher velocities of flow are preferred practically in the design and operation of actual desalination plants due to their effective removal of some types of scale deposits (Monteiro and Airoldi, 1999). The removal rate increased with higher flow velocity due to increased fluid shear stress (Bansal *et al.*, 2000).

Effect of Scale Inhibitor on Deposition of Calcium Sulfate

The effect of Chitosan-DTPA, sodium hexametaphosphate (SHMP) and ethylenediaminetetraacetic acid (EDTA) on the scale formation of calcium sulfate was studied. The concentrations of these scale inhibitors were 1 and 3 ppm.

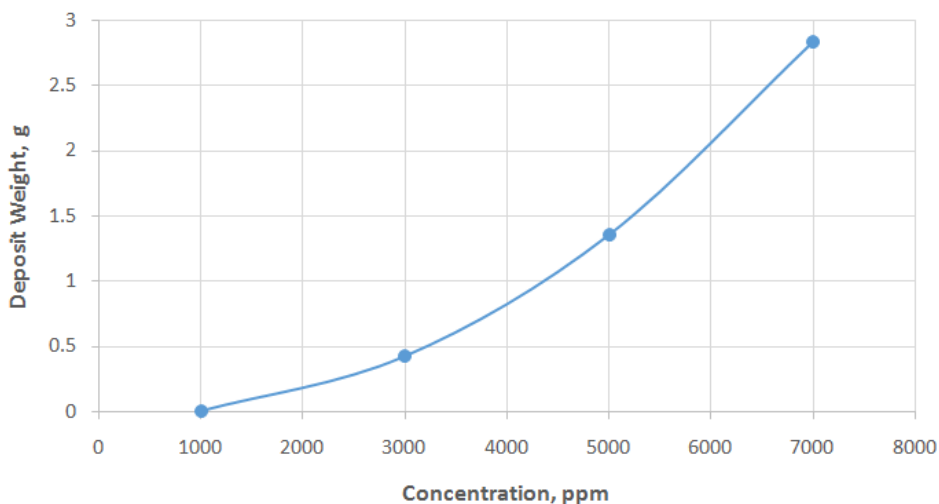


Figure 11. Effect of CaSO₄ Concentration on Deposition Weight. Fixed Conditions: time=72 hr, pH=8, u=0.13 m/s, Re=3000, q=31 Kw/m², T=50 °C

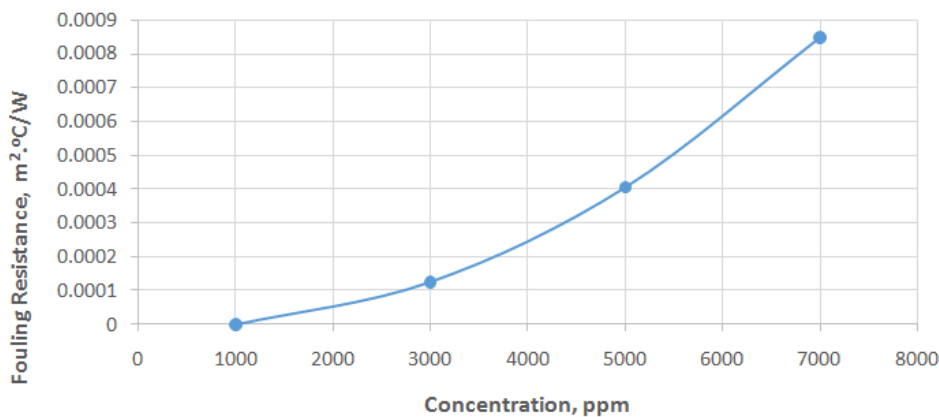


Figure 12. Effect of CaSO₄ concentration on Fouling Resistance. Fixed Conditions: T = 50 °C, Time = 72 hr, pH = 8, u = 0.13 m/s, Re = 3000, q = 31 kw/m²

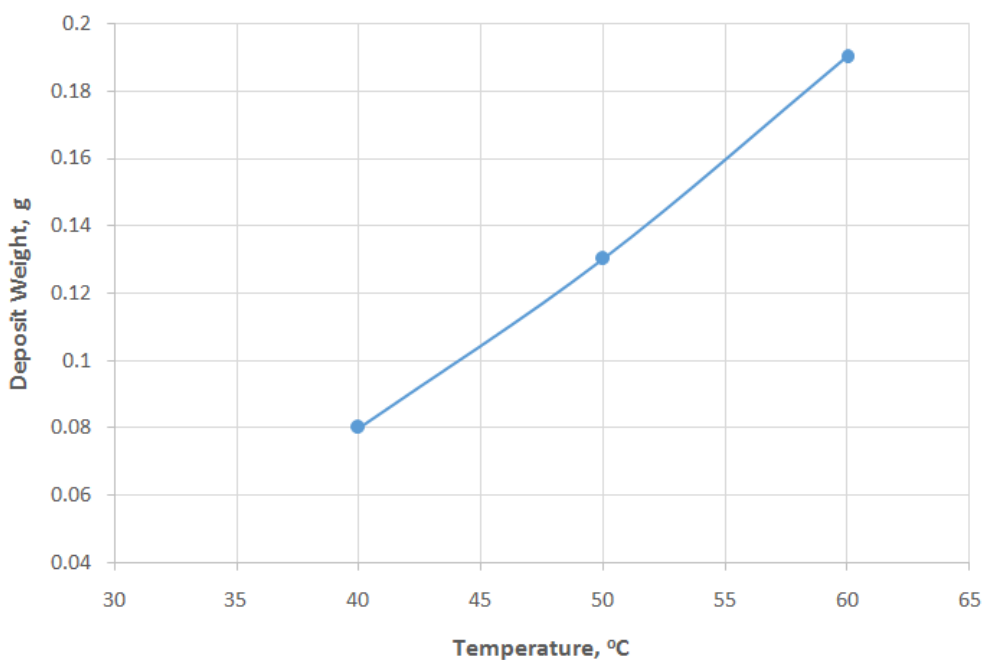


Figure 13. Effect of Temperature on deposition Weight. Fixed Condition: Time = 72 hr, pH = 8, u = 0.087 m/s, Re = 2000, q = 31 kw/m², CaSO₄ Concentration = 1000 ppm

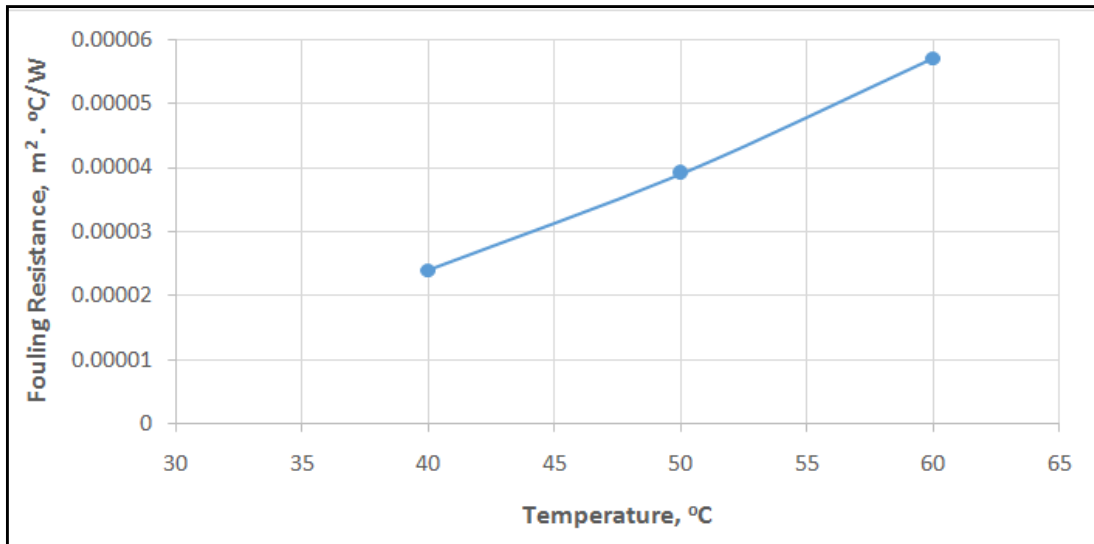


Figure 14. Effect of Temperature on Fouling Resistance. Fixed Conditions: Time = 72 hr, pH = 8, u = 0.087 m/s, Re = 2000, q = 31 kw/m², CaSO₄ Concentration = 1000 ppm

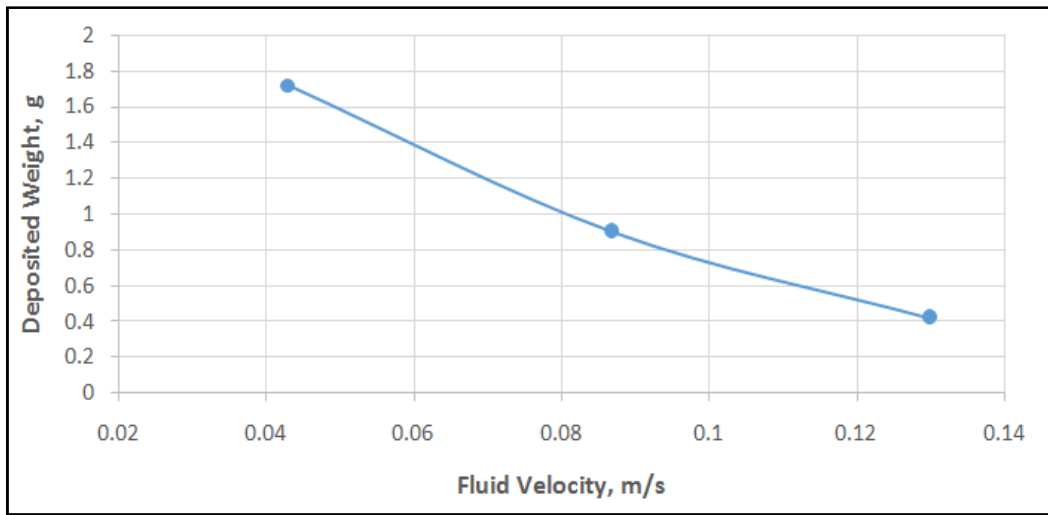


Figure 15. Effect of velocity on deposition Weight. Fixed Conditions: Time = 72 hr, pH = 8, T = 50°C, Re = 2000, q = 31 kw/m², CaSO₄ Concentration = 3000 ppm

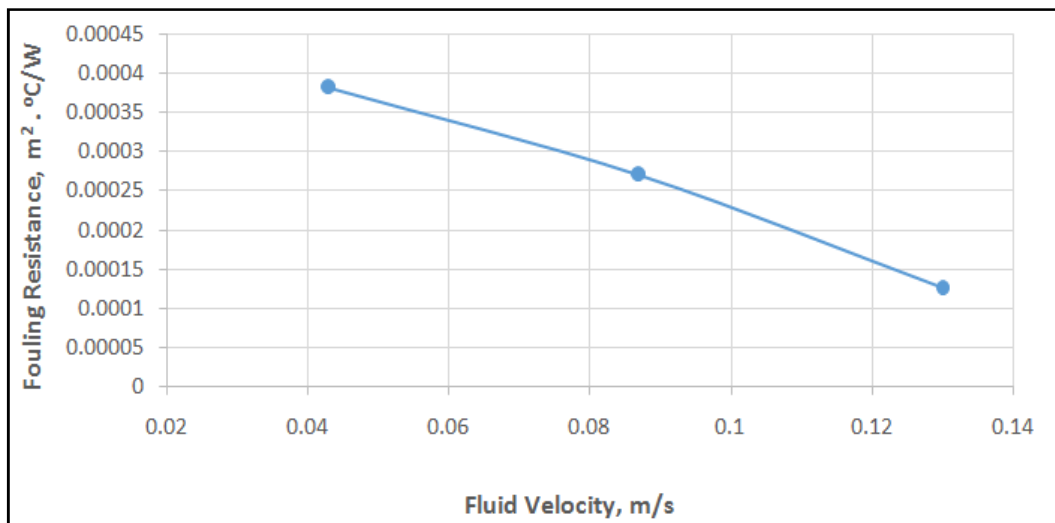


Figure 16. Effect of velocity on Fouling Resistance. Fixed Conditions: Time = 72 hr, pH = 8, T = 50°C, q = 31 kw/m², CaSO₄ Concentration = 3000 ppm

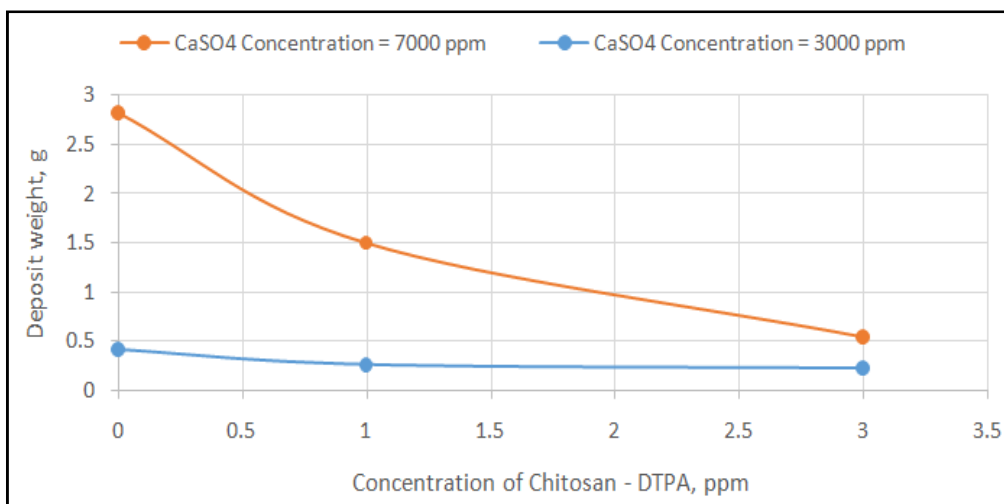


Figure 17. Effect of Chitosan-DTPA Concentration on Deposition Weight. Fixed Conditions: T = 50 °C, Time = 72 hr, pH = 8, u = 0.13 m/s, Re = 3000, q = 31 kw/m²

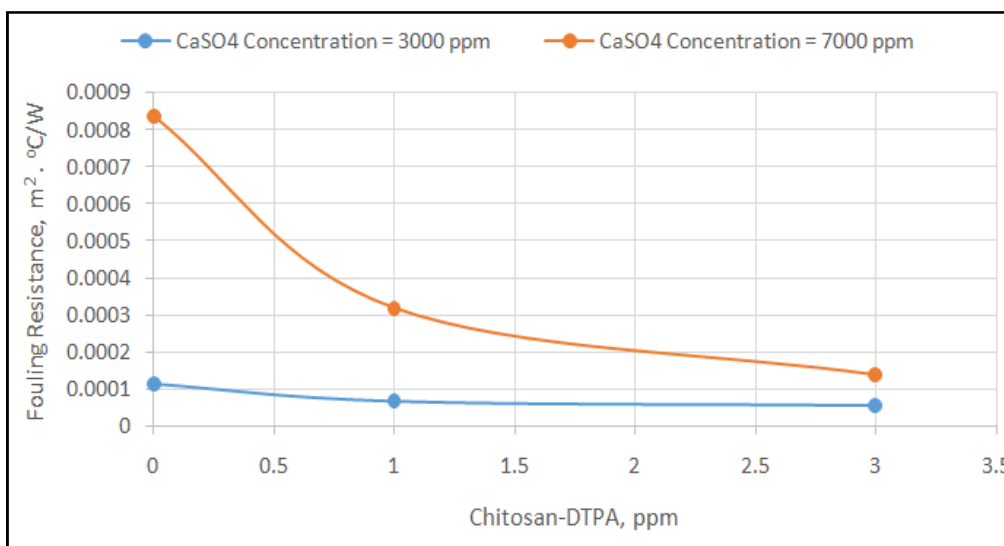


Figure 18. Effect of Chitosan-DTPA Concentration on Fouling Resistance. Fixed Conditions: T = 50 °C, Time = 72 hr, pH = 8, u = 0.13 m/s, Re = 3000, q = 31 kw/m²

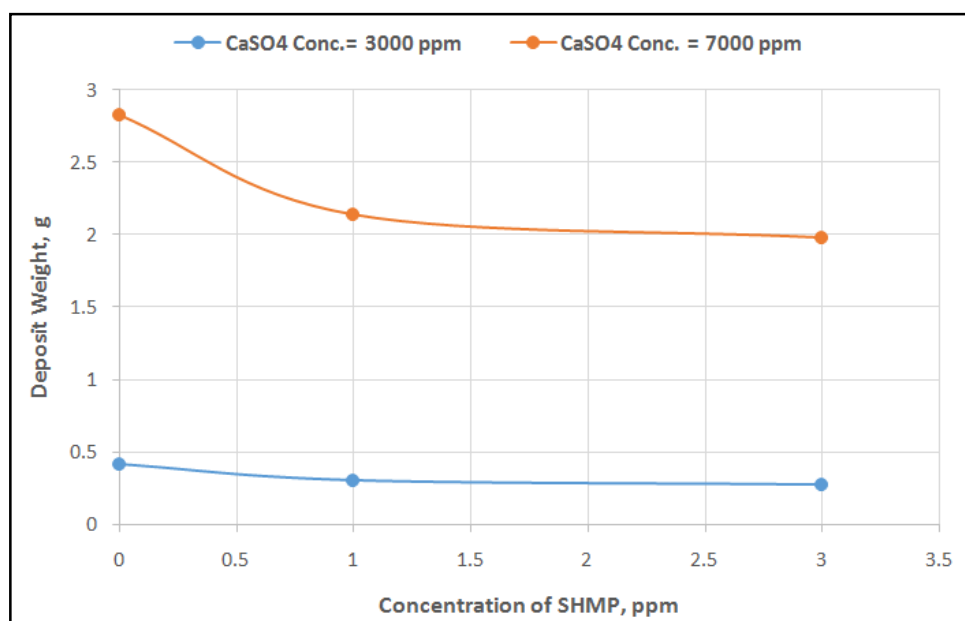


Figure 19. Effect of SHMP Concentration on Deposition Weight. Fixed Conditions: T = 50 °C, Time = 72 hr, pH = 8, u = 0.13 m/s, Re = 3000, q = 31 kw/m²

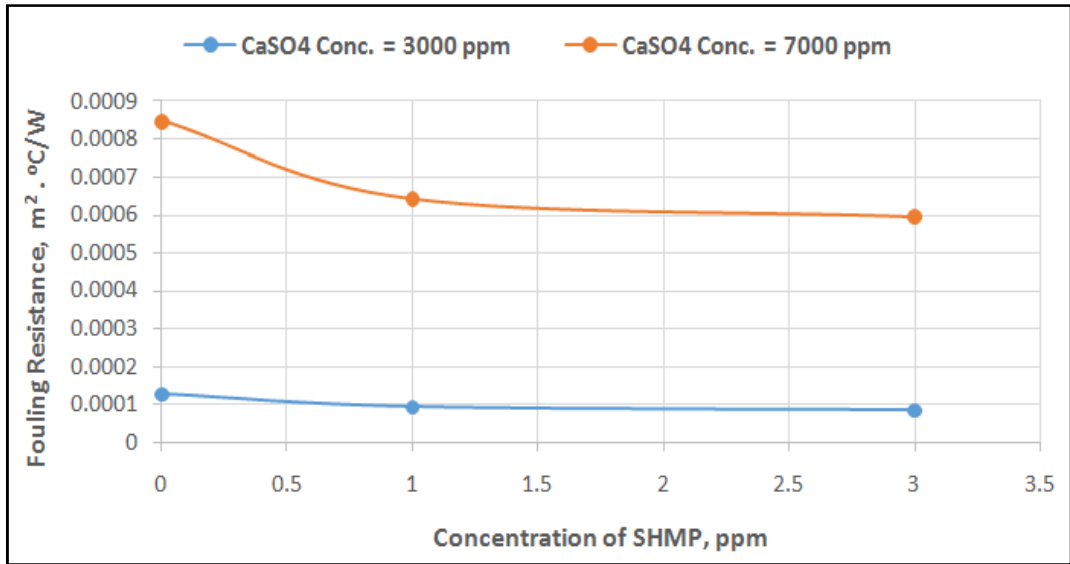


Figure 20. Effect of SHMP Concentration on Foulng Resistance. Fixed Conditions: T = 50 °C, Time = 72 hr, pH = 8, u = 0.13 m/s, Re = 3000, q = 31 kw/m²

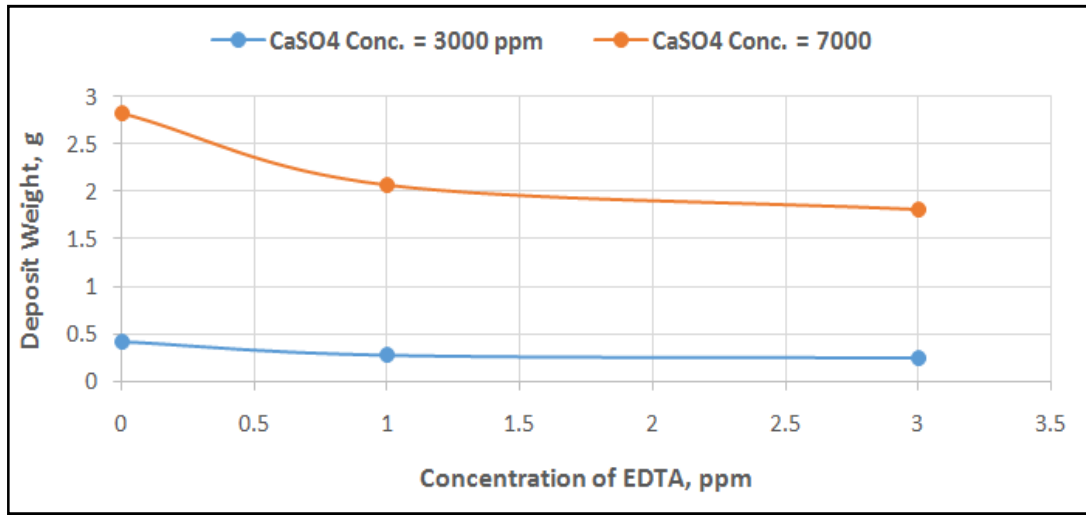


Figure 21. Effect of EDTA Concentration on Deposit Weight. Fixed Conditions: T = 50 °C, Time = 72 hr, pH = 8, u = 0.13 m/s, Re = 3000, q = 31 kw/m²

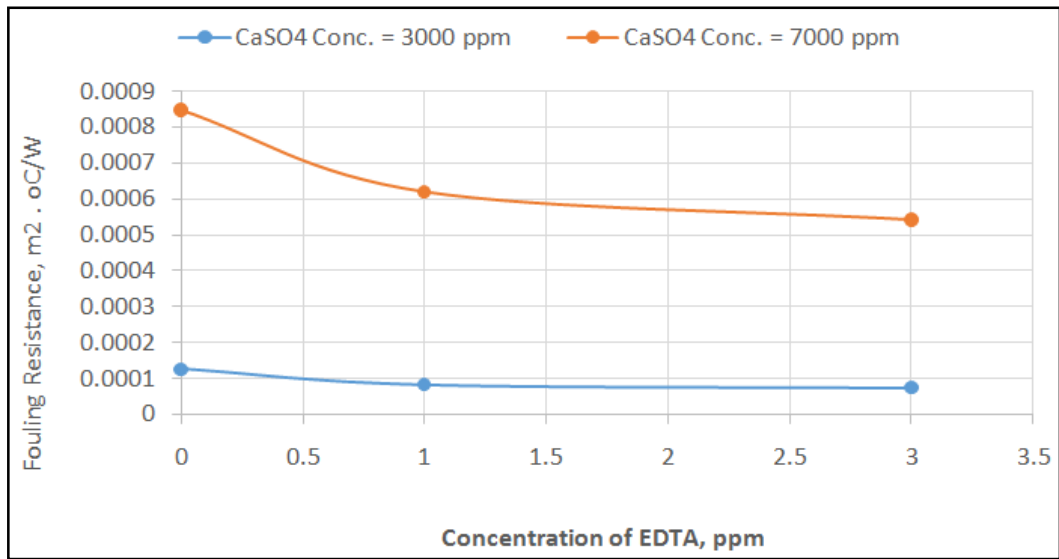


Figure 22. Effect of EDTA Concentration on Foulng Resistance. Fixed Conditions: T = 50 °C, Time = 72 hr, pH = 8, u = 0.13 m/s, Re = 3000, q = 31 kw/m²

Table 3. Effect of scale inhibitors on fouling resistance at the conditions (Concentration of CaSO₄ = 3000 ppm)

Scale inhibitors conc. (ppm)	Fouling Resistance (m ² .°C/W)		
	Chitosan-DTPA	SHMP	EDTA
0	0.000126	0.000126	0.000126
1	0.000067	0.0000931	0.0000841
3	0.000055	0.0000841	0.0000751

Table 4. Effect of scale inhibitors on fouling resistance at the conditions (Concentration of CaSO₄ = 7000 ppm)

Scale inhibitors conc. (ppm)	Fouling Resistance (m ² .°C/W)		
	Chitosan-DTPA	SHMP	EDTA
0	0.000836	0.000847	0.000847
1	0.000576	0.000641	0.00062
3	0.000481	0.000593	0.000542

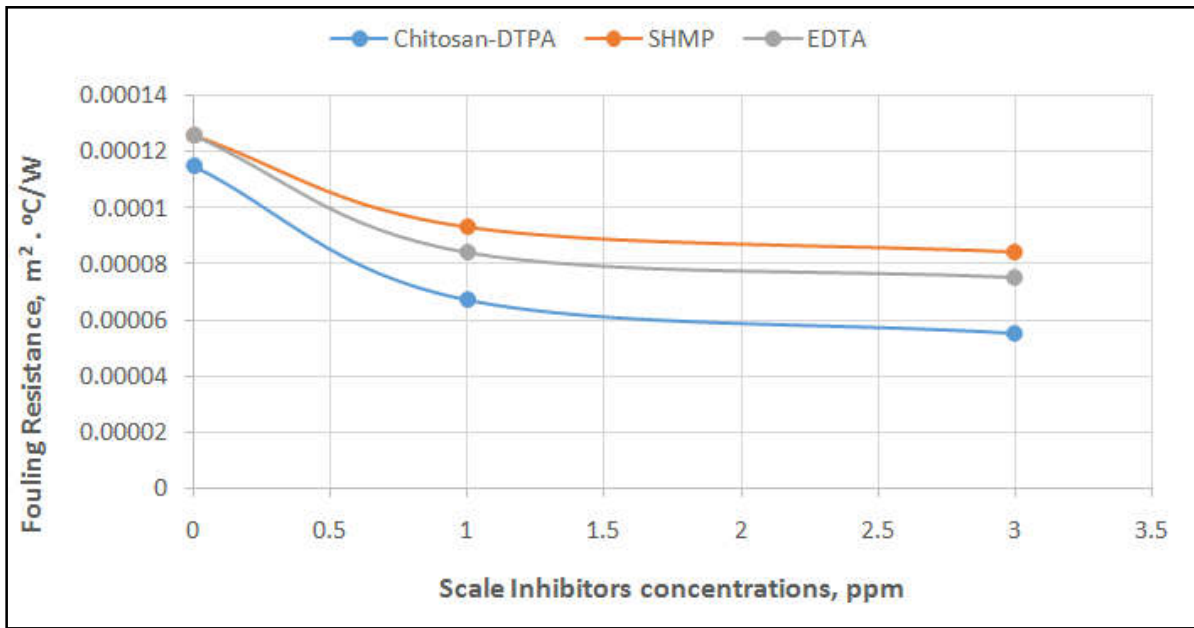


Figure 23. Effect of scale inhibitors on Fouling resistance. Fixed Conditions: T = 50 °C, Time = 72 hr, pH = 8, u = 0.13 m/s, Re = 3000, q = 31 kw/m², CaSO₄ concentration = 3000 ppm

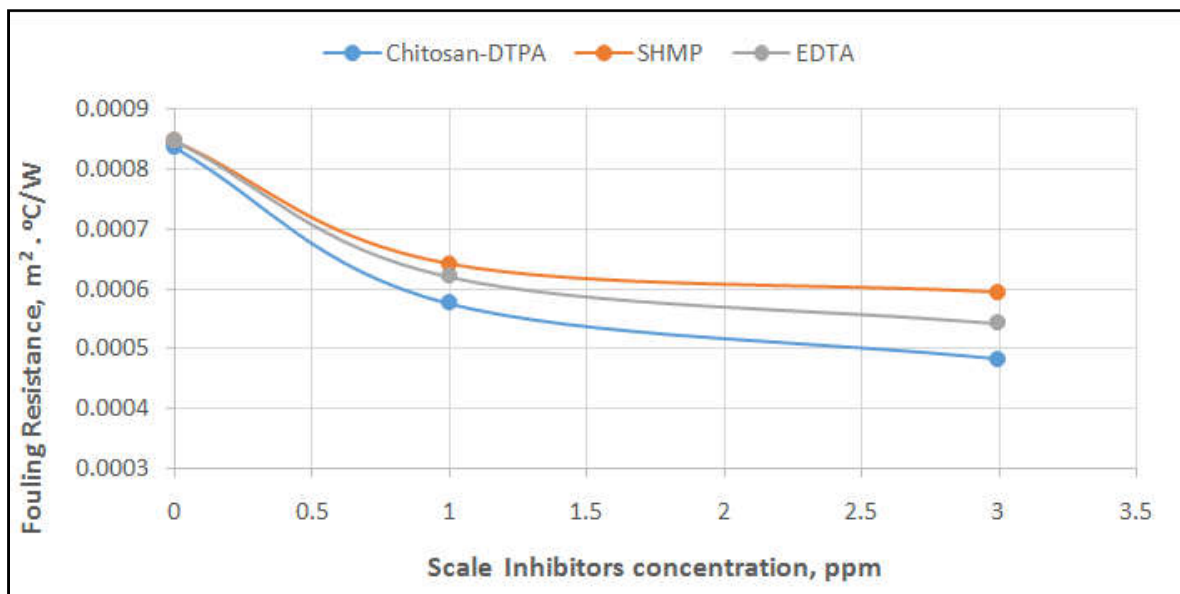


Figure 24. Effect of Scale Inhibitors on Fouling Resistance. Fixed Conditions: T = 50 °C, Time = 72 hr, pH = 8, u = 0.13 m/s, Re = 3000, q = 31 kw/m², CaSO₄ concentration = 7000 ppm

Effect of Chitosan-DTPA

In these experiments, the concentrations of the scale inhibitor used were 1 ppm and 3 ppm. The parameters in this experiment were:

Input Temperature	:	50 °C
Heat Flux	:	31 KW/m ²
pH	:	8
Duration Time	:	72 hr
Fluid Velocity	:	0.13 m/s
Re. No.	:	3000

It is clear from Figs. 17 and 18 that, the fouling deposit and fouling resistance of calcium sulfate decreases by increasing the concentration of the scale inhibitor. The weight deposit is reduced by about 38 % and 31 % when using 1 ppm of Chitosan-DTPA at 3000 ppm and 7000 ppm of calcium sulfate respectively, and about 47 and 42 % when using 3 ppm of Chitosan-DTPA. From these results, it is clear that, the effect of scale inhibitor decreases by increasing the salt concentration.

Effect of Sodium Hexametaphosphate (SHMP)

In these experiments, the concentrations of the scale inhibitor used were 1 ppm and 3 ppm. The parameters in this experiment were:

Input Temperature	:	50 °C
Heat Flux	:	31 KW/m ²
pH	:	8
Duration Time	:	72 hr
Fluid Velocity	:	0.13 m/s
Re. No.	:	3000

It is clear from Figs. 19 and 20 that, the fouling deposit of calcium sulfate decreases by increasing the concentration of the scale inhibitor. The weight deposit is reduced by about 26 % and 24 % when using 1 ppm of SHMP at 3000 ppm and 7000 ppm of calcium sulfate respectively, and about 33 and 30 % when using 3 ppm of SHMP. From these results, it is clear that, the effect of scale inhibitor decreases by increasing the salt concentration. This threshold effect is explained by an adsorption of the inhibitor into the crystal growth site of sub-microscopic crystallites which are initially produced in the supersaturated solution, interfering with crystal growth and altering the morphology of those that grow. Hatch and Rice (Hatch and Rice, 1939) agree with these results. The additive may interfere either with the nucleation or the crystal growth process.

Effect of Ethylenediamene-tetraacetic acid (EDTA)

In these experiments, the concentrations of the scale inhibitor used were 1 ppm and 3 ppm. The parameters in this experiment were:

Input Temperature	:	50 °C
Heat Flux	:	31 KW/m ²
pH	:	8
Duration Time	:	72 hr
Fluid Velocity	:	0.13 m/s
Re. No.	:	3000

It is clear from Figs. 21 and 22 that, the fouling deposit of calcium sulfate decreases by increasing the concentration of the scale inhibitor. The fouling deposit reduces by about 33 % and 27 % when using 1 ppm of EDTA at 3000 ppm and 7000 ppm of calcium sulfate respectively, and about 40 and 36 % when using 3 ppm of EDTA. From these results, it is clear that, the effect of scale inhibitor decreases by increasing the salt concentration. From the previous results and from Tables 3 and 4 and from Figs. 23 and 24 for these scale inhibitor, we can see that Chitosan-DTPA is more effective than the other scale inhibitors to reduce the deposition of calcium sulfate scale at the given conditions. EDTA is more effective than SHMP at the same conditions.

Conclusion

1. The work described in this paper has demonstrated that chitin can be effectively extracted from prawn shells following deproteination using 5% NaOH and demineralisation using 1% HCl.
2. Low molecular mass chitosan samples with DD > 64% and Mw of the major component <10⁴ can be obtained by treating the chitin with 50% NaOH at 100 °C for up to 10 h.
3. The scale formation in water environment is time dependent and has an asymptotic approach.
4. Both concentration of the fouling salt and the fluid temperature as well as the surface temperature affect strongly the calcium sulfate scale formation due to their direct effect on the supersaturation of these fouling salts.
5. The velocity of flow can reduce effectively the calcium sulfate scale deposit (up to 66 %) due to the strong effect on the removal mechanism of the scale layer.
6. The use of scale inhibitor can reduce the scale deposit. Ethylenediamenetetraacetic acid (EDTA) is the most effective in calcium sulfate scale reduction (up to 52%), Ethylenediamenetetraacetic acid (EDTA) reduces up to 40% while sodium hexametaphosphate (SHMP) reduces up to 33%.
7. The antiscalants used in the present work have the following order for reducing calcium sulfate scaling:

Chitosan-DTPA > EDTA > SHMP

REFERENCES

- Abdul Quddus, 2002. "Effect of hydrodynamics on the deposition of CaSO₄ scale on stainless steel", Desalination, 142, 57-63.
- Ahmadi, J., and Steinhagen, M. 1991. "Reduction of Calcium Sulfate Scale Formation During Nucleate Boiling by Addition of EDTA", Heat Transfer Engineering, vol.12, no.4.
- Al-Jalil, S.A.M., 1998. "Experimental Investigation of Scale Formation and Control in Desalination Plants", M.S. Thesis, King Saud University.
- Bansal, B., Müller-Steinhagen, H. M. and Chen, X. D., 2000. "Performance of Plate Heat Exchangers During Calcium Sulfate Fouling- Investigation with an In-line Filter", Chemical Engineering and Processing, vol. 39, pp. 507-519.

- Bipan Bansal, Xiao Dong Chen, Hans Müller-Steinhagen" 2008. Analysis of 'classical' deposition rate law for crystallization fouling", Chemical Engineering and Processing 47; 1201–1210.
- Black C. A ed. 1965. "Methods of Soil Analysis: Part I physical and mineralogical properties" American Society of agronomy, Madison, Wisconsin, 671-698.
- Bott, T.R., *Fouling of Heat Exchangers*. 1995. Elsevier Science & Technology Books. 529. (In-Tech. fouling Mig)
- Darton, E.G. 2000. Desalination 132; 121.
- Faizur Rahman, 2013. "Calcium sulfate precipitation studies with scale inhibitors for reverse osmosis desalination", Desalination 319; 79–84.
- Gazit E., D. Hasson, 1975. "Scale deposition from an evaporating fallingfilm", Desalination 17; 339–351.
- Hasson D., I. Perl, 1981. Scale deposition in a laminar falling-film system, Desalination 37; 279–292
- Hatch, G.B. and Rice, O. 1939. Industrial Engineering Chemistry, 31, 15;
- Heitmann, H.G. 1990. Saline Water processing, VCH, Weinheim.
- KFDA. 1995. Food Additives Code, Seoul: Korea Food and Drug Administration, 449–451.
- Khor E. 2001. Chitin: fulfilling a biomaterials promise. Amsterdam: Elsevier Science.
- Knudsen, J. G. 1990. "Fouling in Heat Exchangers", in "Hemisphere Handbook of heat Exchangers Design", G. F. Hewitt (ed.), Hemisphere.
- Lisitsin D., Q. Yang, D. Hasson, R. Semiat, 2005. Desalination 186; 289.
- Marianna Laka and Svetlana Chernyavskaya, 2006. *Proc. Estonian Acad. Sci. Chem.*, 55(2), 78–84.
- McCrtney, E. R. and Alexander, A. E. 1958. *Journal of Colloid and Interface Science*, vol. 13, pp. 383.
- Monteiro, O.A.C. and Airoidi, C. 1999. Some thermodynamic data on copper-chitin and copper–chitosan biopolymer interactions. *J. Colloid Interface Sci.*, 212, 212–219.
- Muzzarelli RAA, editor. *Natural chelating polymers*. New York: Pergamon.
- Muzzarelli RAA, Jeuniaux C, Gooday GW. 1986. *Chitin in nature and technology*. New York: Plenum; p. 385. Press; 1973.
- Nagib S., K. Inoue, T. Yamaguchi and T. Tamaru, 1999. *Hydrometallurgy*, 51, 73–85.
- Senthilmurugan B., B. Ghosh, S.S. Kundu, M. Haroun, B. Kameshwari, 2010. *Journal of Petroleum Science and Engineering* 75; 189.
- Terbojevidh, M. & Cosani, A. 1997. Molecular weight determination of chitin and chitosan. In *Chitin Handbook* (Muzzarelli, R. A. A. & Peter, M. G., eds). *European Chitin Society*, 87–101.
- Wang, J. C., & Kinsella, J. E., 1976. *J. Food Sci.*, 41, 286–292.
- Yiantsion, S.G., Andritsos, N. and Karabelas, A.J.," 1995. Modeling of Heat Exchanger Fouling: Current Status, problem and Prospects", Engineering Foundation Conferences, New York.
